The relationship between silicate structure and mass transfer of boron in slag refining of silicon

Egil Krystad, Jeffery Kline, Merete Tangstad and Gabriella Tranell
Dept. of Materials Science and Engineering, Norwegian University of Science and Technology, Trondheim, Norway

Abstract: Slag refining of silicon is one of few feasible methods currently in use industrially for removal of boron in the production of silicon for photovoltaic applications. In order to optimize this process, there is a need to enhance the understanding of the relationship between slag composition and the kinetics of boron transfer from metal to slag. In this preliminary work, the kinetics of slag refining using SiO_2-CaO-MgO based slags was studied. Small-scale experiments were performed aiming at comparing the boron mass transfer rate resulting from addition of CaO compared to addition of MgO to SiO_2. A slag composed of 35% CaO and 65% SiO_2 was brought to the molten state together with boron-containing high purity electronic grade silicon in a graphite crucible using a resistance heated tube furnace. The same procedure was carried out using a slag containing 35% MgO and 65% SiO_2. The experiments were performed for a range of durations, after which the content of boron in the silicon could be obtained as a function of time by GDMS analysis. Mass transfer coefficients of boron were determined based on a mass balance consideration of the slag-metal system. The results indicate that the mass transfer rate of boron is higher when CaO is used as the basic constituent for the slag compositions studied. Using Raman spectroscopy, the molecular properties of the oxide structures have been investigated. The obtained mass transfer rates are discussed in light of these findings, assessing the relationship between oxide structure and boron transport through the bulk slag.

Key words: Slag refining, Kinetics, Mass transfer rate, Boron, Solar grade silicon, Raman spectroscopy

1. Introduction

Increasing energy conversion efficiencies and lowered costs in the manufacture of photovoltaic solar modules during the latest decades have made photovoltaic solar power a potential contributor to the world's energy demand. The main photovoltaic material currently used for solar cells is pure crystalline silicon, which is predominantly produced by means of the Siemens process and the related fluidized-bed reactor (FBR) process. The purity of this silicon is higher than the purity necessary for solar cells; moreover, the methods are highly energy intensive. During the last few decades, several processes aiming at producing silicon for photovoltaic purposes by means of pyro-metallurgical methods have been developed in the commercial industry to compete with the Siemens and FBR processes.

Efficient removal of boron is one of the greatest obstacles in the refining of silicon by a metallurgical route. Directional solidification is inefficient due to the high segregation coefficient of boron in silicon; in addition, the vapour pressure of boron is not high enough for removal by vacuum refining. However, removal from silicon by oxidation is possible, and thus the process of slag refining of silicon has been receiving increasing attention as a method for boron removal.

In the slag refining process, boron is removed from the metal when it is oxidized at the metal-slag interface. In

industrial scale solar grade silicon production, the rate at which the refining takes place is of great importance. It is therefore useful to assess the removal rate of boron, as a supplement to the equilibrium boron distribution, which lately has been investigated by several researchers [1-5]. The relationship between slag composition and optimal refining efficiency is still not well known. Better knowledge about the dependence of mass transfer on slag composition can improve the basic understanding of the refining process.

Calcia (CaO) and magnesia (MgO) are common metal oxides added to silica in industrial slag refining. The purpose of the present work is to investigate the relationship between the structure of the silicate slag and the transport of boron from silicon to slag. The mass transfer rate of boron has been empirically assessed. Raman spectroscopy has been used to relate the resulting mass transfer rates to the silicate structure.

2. Theoretical background

2.1 Mass transfer

Oxidation of boron will in practice lead to a variety of boron-oxide compounds in the slag phase. However, since B_2O_3 is the most common boron oxide, the boron-silicon exchange reaction is often represented as

$$B + ¾\ SiO2 = ¾\ Si + BO_{1.5} \quad (1)$$

The total mass transfer coefficient, k_t, depends on several properties at the slag-metal interface: The accumulation of oxidized boron species at the interface is in part attributed to the accessibility of available oxygen bonds in the slag, which is closely related to the network-forming abilities of the particular metal oxide mixture. Following the uptake of boron into the slag, boron-oxide complexes will diffuse through the slag phase. The ratio of basic to acid constituents in the oxide mixture is known as the basicity of the slag. Increasing the basicity will lead to a higher amount of so-called non-bridging oxygens compared to the number of silicate tetrahedra (NBO/T) in the slag structure, which yields a more loosely bound structural network, and in turn alters several physico-chemical slag properties.

2.2 Raman spectroscopy

There are three areas of study inferred from the results of Raman spectroscopy:

1. the study of the forces between atoms in a molecule or compound
2. the study of the structure of the molecule or compound
3. the calculation of thermodynamic entities

Most studies on the structure of silicate melts have been performed by geologists in order to gain an understanding of the nature of the magma in the earth's core. Structural studies of silicate glasses utilizing Raman spectroscopy started as early as the 1930's and continue to the present. A comprehensive review of Raman spectroscopic studies up to 1984 is presented by McMillan, and provides summary of the accepted Raman bands for different silicate compositions [6]. The use of Q^n speciation is utilized in this study to represent the different silicate units. The n denotes the number of bridging oxygen in the silicate unit. High temperature Raman spectroscopic studies have been performed in order to gain insight into the structural changes associated with increasing temperatures. Because the

spectra must be treated for temperature and frequency difficulties in the interpretation of the spectra at high temperatures create uncertainty in the results. Raman spectra associated with glasses is shown to be similar to the spectra obtained for the molten state [7-10] and is chosen as an initial reference point in the study of the structure of silicates.

3. Experimental

3.1 Mass transfer assessment

Slags were created from powdered oxides of CaO, SiO_2, and MgO. In order to minimize effects imposed on the system by trace elements, the metal oxides, silicon and boron used in the experimental work all were of high purity. The oxides were melted to form slags with the desired compositions. Four different slag compositions were created. Also, slag-to-silicon ratios of 1 and 2 were used for two batches of the same slag compositions as a means for controlling the validity of the experimental procedure. The quantities and purity of materials applied in the experimental work are listed in Table 1.

Table 1. Properties and amounts of materials used in the experimental work. S.A.=Sigma Aldrich. M.C.=Merck Chemicals. EG=Electronic grade.

Material	SiO_2	CaO	MgO	Slag total	Si	Boron (in Si)
Supplier	S.A.	S.A.	S.A.	-	Wacker	M.C.
Purity	99.9 %	>99.9 %	>99%	-	9N	99.5%
Fraction size	Powder <44µm	Powder <10µm	Powder <44µm	-	<10mm	Powder ~2µm
Series "SC5050 1:1"	7.5 g (50%)	7.5 g (50%)	-	15 g	15 g	260 ppm
Series "SC5050 2:1"	7.5 g (50%)	7.5 g (50%)	-	20 g	10 g	260 ppm
Series "SCM442"	8 g (40%)	8 g (40%)	4 g (20%)	20 g	10 g	260 ppm
Series "SC6535"	13 g (65%)	7 g (35%)	-	20 g	20 g	290 ppm
Series "SM6535"	13 g (65%)	-	7 g (35%)	20 g	20 g	290 ppm

The melted slag was crushed to fraction size <500 µm. A graphite crucible (Tanso IG-610) with inner diameter 30 mm was used to contain slag and silicon. Silicon was inserted in the crucible and slag was added on top. The crucible was then placed in a vertical resistance-heated tube furnace as shown in Figure 1.

When the pre-determined time had elapsed, crucibles were cooled by turning the furnace off. When cold, each crucible was cut vertically through the center, enabling sampling of the silicon and slag. The reacted silicon was analyzed for boron content by GDMS (EAG Labs, France).

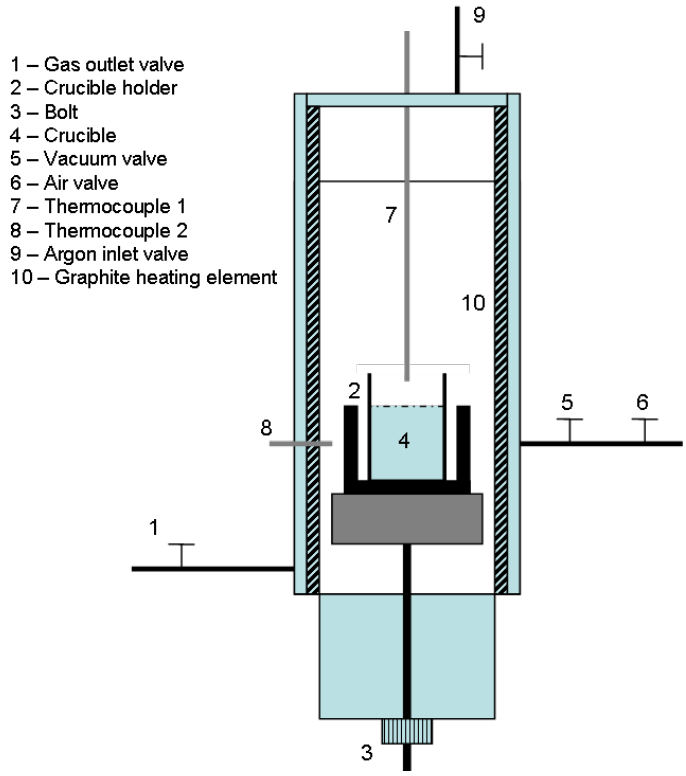

Figure 1. Slag refining experimental setup.

3.2 Raman spectra of metal oxides

Samples of 2g were homogenized and charged into Pt crucibles. A rapid high temperature Kanthal furnace was used for the melting of the glass samples at a temperature of 1600 °C. The samples were held at this temperature for one hour. After one hour holding time, the bottom of the Pt crucible was quenched in cold water to form a glassy sample. The quench rate of ~ 700-400 °C/s was determined by measuring the time it took to hold the crucible in hand from the furnace. Mass loss after melting was 0.04-0.05%.

Raman spectroscopic analysis was performed on a Horiba Jobin Yvon HR800UV system and is shown in Figure 2. A He/Ne laser with a 632 nm wavelength was used as the excitation source. The power of the laser on the sample is 9.4 mW and the diffraction grating is 600 grooves/mm. The intensity of the scattered radiation is taken parallel to the incident beam (IVV). The instrument was calibrated in air and then electronic grade silicon was used as a secondary calibration. Chips of glass are analyzed on carbon wool to assist in orienting the samples flat to the microscope. The measurements were performed under ambient pressure and room temperature.

4. Results

4.1 Mass transfer

GDMS analyses of the silicon contained in crucibles after mass transfer experiments are shown in Figure 2 as a

function of holding duration.

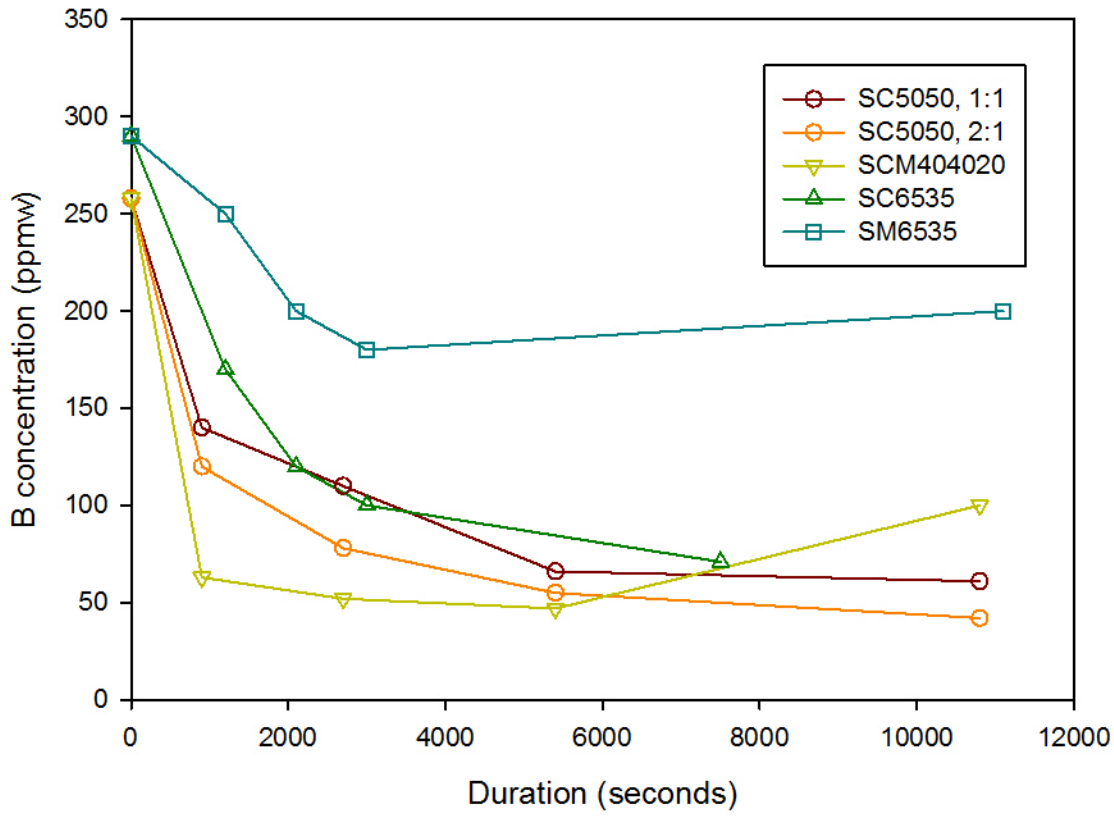

Figure 2. The concentration of boron in the silicon from GDMS analyses.

The mass balance of boron combined with Fick's 1st law yield a differential equation which will result in the following expression for the boron concentration in silicon at a given holding duration t:

$$\frac{[\%B]-[\%B]_e}{[\%B]_{in}-[\%B]_e}=\exp\left\{-\frac{\rho k_t A_s t}{M}\left(1+\frac{\gamma_B}{Kf_B}\frac{M}{M_s}\right)\right\} \tag{2}$$

where

M and M_S (kg) are the mass of silicon and slag, respectively;

[%B] is the boron content in silicon;

A_s (m^2) is the interfacial area between silicon and slag.

Subscripts *e* and *in* denote equilibrium and initial concentrations, ρ is the metal density, γ_B and f_B are the equilibrium coefficients of B in slag and silicon, and K is the equilibrium constant of the oxidation reaction.

The partition ratio, commonly denoted L_B, is the ratio between slag and metal concentrations of boron at equilibrium. If assumed negligible boron content in the slag before the mass transfer process, we have

$$L_B=\frac{(\%B)_e}{[\%B]_e}=\frac{M_{Si}}{M_{slag}}\frac{[\%B]_0-[\%B]_e}{[\%B]_e} \tag{4}$$

The equilibrium constant is given by

$$K = \frac{(\%B)_e \gamma_B}{[\%B]_e f_B} = L_B \frac{\gamma_B}{f_B} \tag{3}$$

where round brackets denote boron concentration in slag and square brackets, boron concentration in metal. By rearranging the equations above we obtain a relationship between the mass transfer coefficient and time:

$$\frac{M}{\rho A_s \left(1 + \frac{M}{L_B M_S}\right)} \ln \frac{[\%B] - [\%B]_e}{[\%B]_{in} - [\%B]_e} = -k_t \cdot t \tag{5}$$

For simplicity this may be represented as

$$Y \ln X = -k_t \cdot t \tag{6}$$

After solidification, the silicon piece in each crucible was found to have formed a near-spherical shape. The interface area between silicon and slag varied according to the amount of slag and silicon used in the experiments. For simplicity, the evaporation of slag from the crucibles when at the molten state was disregarded and the area A_s was calculated from geometric considerations of the near-spherical silicon lump. Figure 3 shows the product Y·lnX for the boron concentration achieved in the present work and the resulting linear regression slopes. The mass transfer coefficient values are summarized in Table 2..

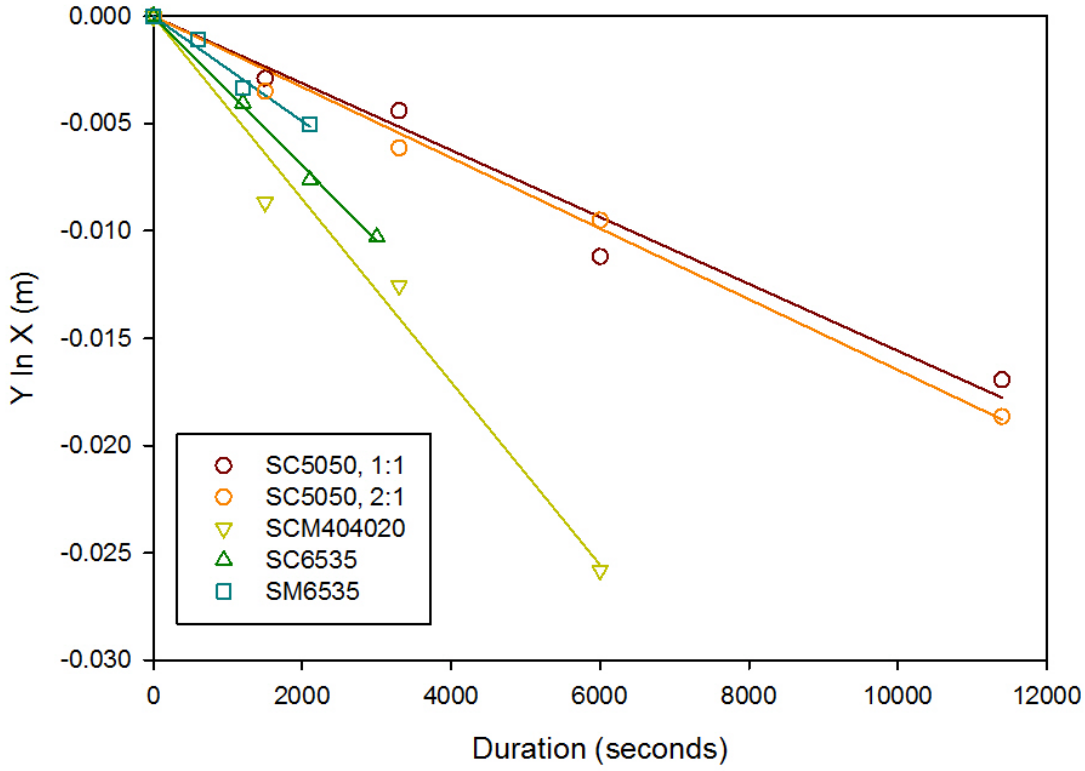

Figure 3. Plot of the left side of Eq. (6), as a function of time.

Table 2. Values of k_t and L_B calculated from the mass transfer series

Series	k_t (10^{-6} m/s)	L_B
SC 50:50; Slag:Si 1:1	1.8	3.3
SC 50:50; Slag:Si 2:1	1.7	2.6
SCM 40:40:20; Slag:Si 2:1	4.3	2.3
SC 65:35	3.5	3.1
SM 65:35	2.5	0.9

4.2 Raman spectroscopy

Minor differences occur at the 1050 cm^{-1} region (Q^3) where the steepness of the shoulder increases with increasing MgO content as illustrated in Figure 4. Maintaining the SiO_2 at a constant 65 wt% and decreasing the CaO content in the MgO system destroys the 600 cm^{-1} Raman band (three-member ring). A new band forms near 550cm^{-1} and increases in intensity with increasing concentration of MgO.

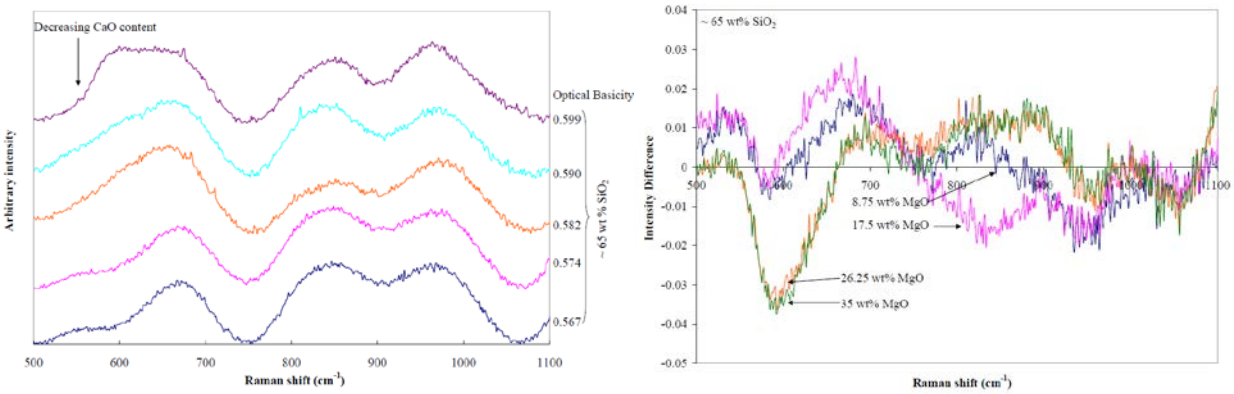

Figure 4. Raman spectra in the CaO-MgO-SiO_2 system with ~ 65 wt% SiO_2 on the left and a plot of CaO spectra subtracted from the MgO spectra at ~65 wt% SiO_2 is displayed on the right.

For a more complete understanding of the structural differences with the substitution of CaO with MgO the spectrum of the CaO was subtracted from the spectra of the MgO series and is illustrated in Figure 4. The low frequency region verifies the decrease in concentration of the three-membered ring with substitution of CaO with MgO. An increase in the Q^1 species is observed in the high frequency region with increasing MgO content.

The addition of B_2O_3 to both the MgO and CaO systems exposes how B_2O_3 behaves in the different structural environments. The difference spectra for both the CaO and MgO systems are displayed in Figure 5. The band near 700 cm^{-1} increases with the addition of B_2O_3. There is an increase in the 800-850 cm^{-1} area with the addition of B_2O_3. A decrease in the other Q^n species is observed with the addition B_2O_3. A noticeable decrease in the three-membered ring (600 cm^{-1}) results with the addition of B_2O_3 to the CaO system. The Q^n species region experiences an increase with the addition of B_2O_3.

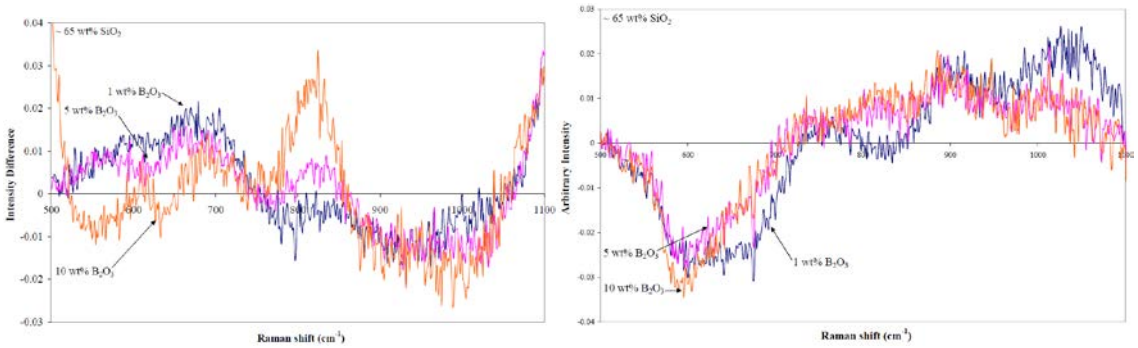

Figure 5. Difference spectra of the MgO doped with B_2O_3 on the left and the difference spectra of the CaO doped with B_2O_3 on the right.

5. Discussion

The uncertainty in the results from mass transfer experiments is rather large, partly due to the small number of measure points. Also, it is highly possible that a high degree of SiO_2 evaporation has occurred during the experiments of long holding durations, and that this has caused formation of solid oxide phases causing change in the boron uptake properties. The series "SCM 40-40-20", in particular, shows an incline in boron concentration at long holding duration. However, clear trends can be seen in Figure 2 regarding the boron concentration in the silicon phase and the subsequent discussion therefore assumes the data obtained to be sufficiently consistent.

The series "SCM" shows the best refining efficiency of the slags researched in this work with regard to the rate of removal. This series constitutes the highest amount of basic to acid slag constituents, and thus a higher NBO/T ratio than for the other slags applied. Moreover, it is seen that the mass transfer coefficient is similar for the two series denoted "SC5050", where the slag-silicon ratio is 1 and 2, respectively. Hence the difference in slag to metal ratio does not seem to play a significant role for the calculated mass transfer rate. It is also easily observed that the series "SC 6535" exhibits a higher mass transfer rate than the series "SM 6535". The calculated L_B values are between 2.3 and 3.3 for all series shown in Table 2 except the series "SM 65:35" which exhibited a substantially higher equilibrium boron concentration in silicon and thus a low L_B value.

McMillan proposed a structural model suggesting the larger cation would prefer the Q^3 unit and the smaller cation would prefer the Q^2 unit at given silica content [9]. The study of Na_2O-CaO-SiO_2 glasses indicates a preference of the Ca^{2+} cation to bond with the NBO associated with the Q^2 structure, and Na^{1+} prefers the Q^3 structural unit [11]. An implication of these studies is the larger field strength metal cation will tend to bond with the oxygen in the most depolymerized structural unit (Q^n).

Steric hindrance related to the Q^2 species should prefer the small cations compared with the large Ca^{2+}. A chemical reaction scheme is suggested to express the silicate distribution and is shown in Equation 7 [9].

$$2Q^3 = Q^4 + Q^2 \quad (7)$$

According to the proposed species preference, the larger cations will favor a reaction to the left and smaller cation will drive the reaction to the right. This is supported by the decrease in Q^3 speciation upon addition of MgO; however,

the proportion of Q^2 species is essentially unchanged with the initial increase in MgO content as observed in Figure 2. Exchanging CaO with MgO at constant 65 wt% SiO_2 shows little effect on the relative distribution of the Q^0 and Q^2 speciation. The larger charge concentration ascribed to the Q^1 species appears to prefer the smaller cation with a larger charge to radius ratio. Neglecting the contribution of the Q^3 unit to the total structure and focusing on the dominate species suggests a disproportionation reaction mechanism displayed in Equation 8.

$$2Q^1 = Q^2 + Q^0 \quad (8)$$

A mechanism with the required composition of Equation 8 implies silicate anions related to Q^1, Q^2 and Q^0 as $Si_2O_7^{6-}$, SiO_4^{4-} and $Si_4O_{12}^{8-}$ respectively.

The use of optical basicity instead of NBO/T is due to the inability to determine a fraction of B^{3+} in the tetrahedral coordination. The band near 808 cm^{-1} is assigned to the breathing vibration of the boroxol group and increases in relative intensity with increasing B_2O_3 [12]. The low frequency region in the CaO system is dominated by the 650 and 670 cm^{-1} defect bands and the 600 cm^{-1} three-member ring. A three-member ring is strained compared to a four-member ring. Oxygen atoms in the silicon tetrahedron have a larger electronegativity and experience a partial negative charge while the silicon will have a partial positive charge. The formation of a three-member ring results in silicon to expose the empty d-orbitals producing a more acidic silicon atom [13]. A transfer of electrons to the oxygen results in the oxygen becoming more basic according to Lewis acid base theory. Addition of B^{3+} to the system should preferentially react with the more basic oxygen to form a lower energy structure.

It has been proposed that the three-member rings occupy the surface sites [14]. The presence of the 600 cm^{-1} band corresponding to the three-member ring in the CaO system may indicate B^{3+}, as trigonal coordination, is reacting with the more basic oxygen in the ring distorting the structure. The difference spectra illustrate the decrease in the 600 cm^{-1} band with the addition of B_2O_3 supporting this proposal.

The increase in the 800-850 cm^{-1} region in the MgO system indicates the possible formation of the boroxol unit. This increase contains contributions from both the formation of the Q^0 species and the boroxol unit. The decrease in the other Q^n species is likely due to a reaction with B_2O_3 forming the Q^0 species.

6. Conclusions

The work carried out on mass transfer rates indicate that CaO as slag constituent will promote transport of boron from silicon to slag in comparison with MgO. Substituting MgO for CaO in a SiO_2-MgO slag with composition 65:35 will lead to a 40% increase in mass transfer coefficient, from 2.5 to 3.5 μm/s. This fits with the findings of the experimental work done on Raman spectra. The presence of the three-membered ring in the CaO system combined with the surface activity associated with the three-membered ring creates an environment conducive for the uptake of boron into the slag phase. The destruction of the three-membered ring upon addition of B_2O_3 indicates a reaction between the two species. A lack of ring structures in the MgO system results in B_2O_3 combining with the more polymerized Q^n species. This reaction produces an increase in the less polymerized Q^0 unit.

References

[1] Cai, J., et al., Boron removal from metallurgical silicon using CaO-SiO2-CaF2 slags. *Transactions of Nonferrous Metals Society of China*, 2011. **21**(6): p. 1402-1406.

[2] Johnston, M.D. and M. Barati, Distribution of impurity elements in slag-silicon equilibria for oxidative refining of metallurgical silicon for solar cell applications. *Solar Energy Materials and Solar Cells*, 2010. **94**(12): p. 2085-2090.

[3] Morita, K. and T. Miki, Thermodynamics of solar-grade-silicon refining. *Intermetallics*, 2003. **11**(11-12): p. 1111-1117.

[4] Teixeira, L.A.V., et al., Behavior and State of Boron in CaO-SiO2 Slags during Refining of Solar Grade Silicon. *Isij International*, 2009. **49**(6): p. 777-782.

[5] Luo, D.-w., et al., Removal of boron from metallurgical grade silicon by electromagnetic induction slag melting. *Transactions of Nonferrous Metals Society of China*, 2011. **21**(5): p. 1178-1184.

[6] McMillan, P. Structural studies of silicate glasses and melts-applications and limitations of Raman spectroscopy, *American Mineralogist*, **69**(1984), 622-644.

[7] Seifert, F., Mysen, B., and Virgo, D. Structural similarity of glasses and melts relevant to petrological processes, *Geochimica et Cosmochimica Acta*, **45** (1981), 1879-1884.

[8] Mysen, B. The Structure of Silicate Melts, *Annual Review of Earth and Planetary Sciences*, 11(1983), 75-97.

[9] P. McMillan, A Raman, Spectroscopic Study of Glasses in the System CaO-MgO-SiO_2, *American Mineralogist*, **69** (1984), 645-659.

[10] Osipova, L., Osipov, A., and Bykov, V. Structure of B_2O_3 Melt by Raman Spectroscopy, *Informational Bulletin of the Annual Seminar of Experimental Mineralogy, Petrology and Geochemistry*, (2003) 1-2.

[11] Jones, A.R., Winter, R., Greaves, G.N., and Smith, I.H. MAS NMR study of soda-lime-silicate glasses with variable degree of polymerization, *Journal of Non-Crystalline Solids*, **293-295** (2001), 87-92.

[12] J. Krogh-Moe, The Structure of Vitreous and Liquid Boron Oxide, *Journal of Non-Crystalline Solids*, **1** (1969), 269-284.

[13] P. Boudjouk, C. Kapfer, and R. Cunico, Synthesis and Reactivity of 1-Silaadamantyl Systems, *Organometallics*, **2** (1983), 336-343.

[14] C. Brinker, R. Kirkpatrick, D. Tallant, B. Bunker, and B. Montez, NMR Confirmation of Strained “Defects” in Amorphous Silica, *Journal of Non-Crystalline Solids*, **99** (1988), 418-428.